

Possibilities and Limitations in the extrinsic Synchronization of Observations from Networks of Robotic Total Stations

Gabriel KEREKES, Volker SCHWIEGER, Germany

Key words: Streaming, Robot positioning, Synchronization, Simultaneity, RTS-Network

SUMMARY

High-precision, real-time positioning is a critical aspect of automation in the construction industry. Especially for the collaborative control of multiple manipulators or robots, absolute positioning within mm accuracy is often required. One way to provide absolute positions in real time is to use robotic total stations (RTSs). Although they are indispensable on most construction sites and are often used for tracking purposes (e.g. in machine control), networks of multiple RTSs are rarely used. In addition to providing positioning redundancy, RTS networks can help ensure the uninterrupted flow of the automated process. This can only be achieved if a common temporal and spatial frame is available for all the RTSs in the network. The common spatial reference frame is self-explanatory and easy to achieve, but the common temporal frame is challenging. This paper presents an approach for synchronizing observations from a RTS network. This will be referred to as the extrinsic synchronization. Four Trimble S7 RTSs are used in this network and the time frame is provided by an NTP server. The possibilities for synchronizing observations streamed at 10 Hz and 20 Hz are exemplified using reflectors mounted on a rotating arm. Two different scenarios are presented with angles combined with distance measurements and angle measurements only. Simultaneous measurements are possible if synchronization between the four RTSs is realized. The achieved simultaneity is around 0.3 ms between measurements of four individual RTS. This means that even at speeds up to 2.5 m/s, the error induced by this delay remains theoretically in sub-mm level. Limitations of this type of network are related to the hardware capabilities of the RTSs and the external control software.

Possibilities and Limitations in the extrinsic Synchronization of Observations from Networks of Robotic Total Stations

Gabriel KEREKES, Volker SCHWIEGER, Germany

1. INTRODUCTION

Currently, the construction sector is facing major challenges, such as the high demand for living spaces, the need for rapid extension and development of infrastructure works, and the shortage of skilled workers. To address some of these issues, efforts are being made to automate processes in construction (Knippers et al., 2021), as it is one of the least digitized and automated sectors worldwide. However, automating repetitive tasks in the construction industry is not as straightforward as in other industrial sectors where robots and machines have fixed positions, such as on a production line. The construction industry requires a more flexible solution for the positioning of manipulators and the handling of materials and components (Lauer et al., 2023). Facing these challenges is a first step in increasing productivity (Knippers et al., 2021). This research paper addresses one of these challenges within the Cluster of Excellence Integrative Computational Design and Construction for Architecture (IntCDC), by taking essential steps towards automated cyber-physical construction processes.

In general, positioning is a crucial aspect of automation in the construction, particularly for the collaborative control of multiple manipulators or robots (cf. Corke, 2017). Absolute positioning within millimeter accuracy is often necessary. One way to provide absolute positions in real time is to use robotic total stations (RTSs). These polar measurement systems can provide 3D position of single points (signalized or not) in a given coordinate system. Although RTSs are versatile and ubiquitous on most construction sites, their full potential has not yet been fully harnessed. In most applications, RTSs are used for surveying, staking out or for tracking purposes (e.g. in machine control), but usually one RTS is sufficient for these tasks. Networks of multiple RTSs that work simultaneously are rarely used. This is understandable, since RTSs with tracking capabilities are usually high-end, expensive, measurement instruments. However, networks of RTS provide positioning redundancy and ensure an uninterrupted process of the respective automation even if the line of sight of some (not all) RTSs is interrupted by an obstacle (Kerekes & Schwieger, 2018).

The first examples of polar measurement instruments networks date back to those theodolite measurement systems (TMS) (cf. Bill, 1985) used in industrial measurements. Since then, technology has rapidly evolved, resulting in commercially available RTSs capable of accurately measuring up to 20 positions per second while the target is moving (Schwieger et al., 2020; Stempfhuber & Sukale, 2017; Ehrhart & Lienhart, 2017). In order to achieve this, a RTS relies on multiple sensors that need to perform tasks simultaneously (cf. Kleemaier, 2018). However, this can be challenging due to internal hardware and software limitations, problem commonly referred to as synchronization error. This is also known as the intrinsic (internal) synchronization. Many publications deal with this topic (cf. Stempfhuber, 2004; Vogel et al.,

2023; Thalmann & Neuner, 2021; Kleemainer, 2018; Gojčič et al., 2017). However, none of these can be considered generally applicable to all RTS, as each manufacturer employs different architectures and approaches to minimize the effects of the synchronization errors. The above-mentioned publications only address Leica RTSs (Leica Geosystems AG) and the suggested synchronization routines may not be entirely applicable to instruments from other manufacturers, although the problem remains the same. There are some exceptions and it is promising that researchers are also using Trimble RTS for similar research (Vaidis et al., 2021; Horeličan, 2021; Vaidis et al., 2022). In any case, efforts are made in both the scientific and industrial communities to overcome this unsatisfactory situation. These efforts are justified, since according to the recently published market overview for RTS, an exponential market growth is predicted within the years 2023 to 2030 (Verified Market Reports, 2023).

The current contribution does not address the intrinsic synchronization. Instead, the focus is set on the extrinsic synchronization and simultaneous measurements between several RTSs. Note that in this publication, the authors use the terms “synchronization” for measurements obtained within the same temporal reference frame and the term “simultaneity” for measurements take at the same time (quasi-simultaneity). This means that measurements obtained from each RTS can only be simultaneous, if the RTSs are synchronized.

A previous publication on the topic, Lerke & Schwieger (2021) presented theoretical aspects and investigated the achievable geometrical positioning quality in a system composed of four RTSs evenly distributed in space that should aid in robot control. The study is based solely on simulations, and the network of RTSs has not been evaluated in a real kinematic scenario. Continuing this line of work, the current test scenarios aim to improve the existing RTS network at the Institute of Engineering Geodesy (IIGS) within IntCDC. Four Trimble S7 (Trimble Inc., 2018) RTS are used, along with another Software Development Kit (SDK) under a Linux OS. Additionally, the common reference frame is established by constantly updating the system time of the Linux OS via an NTP server. To evaluate the temporal and geometrical positioning quality, a moving object is tracked with 10 Hz and 20 Hz under laboratory conditions. Reference values for the geometry are determined with an API Radian laser tracker. The chosen speeds of the moving object were based on the technical specifications of robots that will be used in IntCDC in the future.

2. DESIGN AND REQUIREMENTS OF A RTS NETWORK

2.1 Network design

For real-time positioning tasks, an RTS network must meet several conditions, including:

- delivering coordinates in the same spatial reference frame;
- working with the same time reference frame;
- measuring at a constant sampling rate;
- reliably tracking a moving reflector in both horizontal and vertical direction.

Based on these criteria, a network of RTS was designed at the IIGS using four RTSs. The system consists of four Trimble S7 RTS, four Raspberry Pi (RasPi) 3B+ running under Raspbian OS and a central host laptop running under Windows OS (Fig. 1). Only the necessary technical specifications are listed here for completeness.

The used S7 instruments are all high-end RTS with 0.3 mgon angle measurement accuracy for single measurements, finelock pointing precision of < 1 mm at 300 m limiting the angle accuracy in this range, $\sqrt{(4 \text{ mm})^2 + (2 \text{ ppm})^2}$ distance measurement accuracy (RMS) in tracking mode, the electromagnetic direct drive for the servo/angles sensors and can reach a maximum rotation speed of 128 gon/sec (Trimble Inc., 2018). In tracking mode, the angle measurement accuracy is not specified in the datasheet of the S7, however, comparing the specifications with other Trimble RTS (e.g. SPS930), the angle measurement accuracy in tracking mode is known to be double as the one in static mode (cf. Trimble Inc., 2008). The finelock accuracy will consequently be valid up to 300 m. The instrument's capability to track moving objects is referred to as Advanced Tracking Sensor (ATS) and internal synchronization between measurements is realized with less than 1 ms (Trimble Inc., 2008). Additionally, the S7 can automatically find and track active and passive reflectors (prisms), especially the Trimble own reflectors like the Trimble MT1000 MultiTrack target up to 800 m. This reflector consists out of eight individual prisms assembled together.

The network is intended for application on construction sites, which means that the communication between each RTS and central host must be assured at all times, independent of local obstructions or interferences from other wireless devices (e.g. those that use Radio or WLAN). Moreover, the majority of RTS can be connected to a terminal by a serial cable (including USB), but for all these cables there is a limitation for the cable length based on data streaming rate for RS-232 cables or USB cables, e.g. up to 5 m, without any special amplification (Axelson, 2007). Therefore, the standard included 6pin to USB 1.2 m cable used for connecting a controller or computer with the RTS cannot be simply extended by a longer USB cable. A workaround is to connect the instrument via USB cable to a Raspberry Pi and then pass the streamed data forward to the central host via LAN cable. This solves one of the hardware limitations, because LAN cables (RJ45) can be longer without loss of baud rate. The used LAN cables in this network are 100 m long for each RTS. They are all connected to a LAN switch, which is additionally connected to the internet and the host computer.

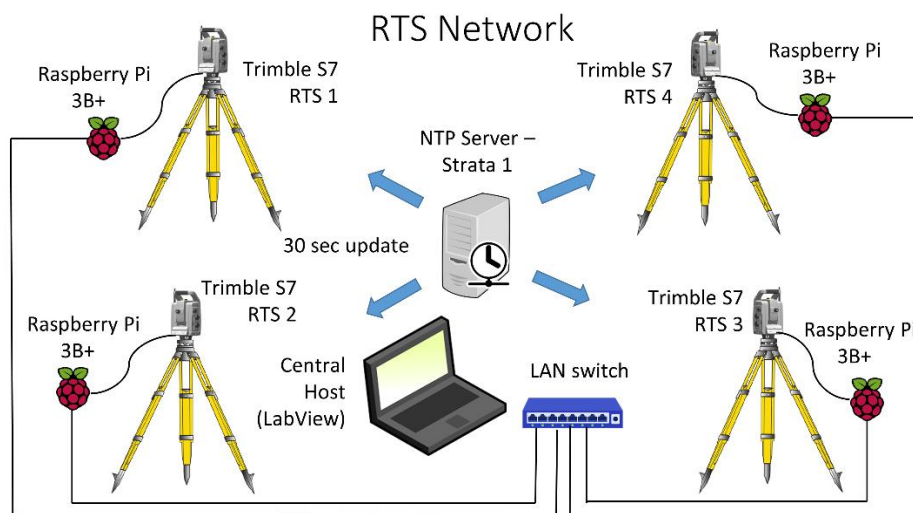


Figure 1 System overview of the RTS network realized at the IIGS within IntCDC.

In order to send and receive data from the S7 RTS and central host, the Trimble Linux SDK must be installed on the RasPis and custom scripts written in C++ must run during the operation time. This SDK was developed for single board computers that have the ARM (Advanced RISC Machines) system architecture. This is also the reason for using the RasPi in the first place. The C++ script starts a server application on each RasPi, which accepts commands, which can be directly sent to the RasPis IP address. The communication is bidirectional; therefore, streamed measurements can be read from the same IP address.

The time stamps attributed to each measurement are timestamps of the respective OS, in this case the respective RasPi. Unlike other single board computers, the RasPi 3 model B+ does not have a Real Time Clock (RTC) module that most portable devices have to keep track of time when shut down (Jolles, 2021). If not connected to the internet, the system time will be local time and will drift slowly during operation as time passes. An internet connection is required for synchronizing the system time with the help of network time protocol (NTP) servers. This feature is used in the current RTS network in order to create the same time frame for the streamed data. All RasPis update their time constantly at the minimum poll interval each 32 s from an NTP Strata 1 Server of the University of Stuttgart (rustime01.rus.uni-stuttgart.de). The precision for the updated NTP time is 1 μ s as declared in each NTP message (cf. Martin et al., 2010).

On the central host, a LabView code was developed to assure the communication between all RasPis. LabView was chosen due to simplicity and possibilities of parallelizing control loops. In the code, data is sent and received at the TCP/IP ports of the RasPis. Additionally, the previously mentioned C++ scripts that must run on the RasPis can be remotely started from the host computer through a terminal emulator, e.g. PuTTY.

2.2 Requirements of the RTS network

Up to now, the RTS network design was explained. As regards the requirements for tracking objects travelling at different speeds, a table is established based on the speeds encountered in future applications. The lowest (0.15 m/s) and highest (2.5 m/s) speeds are from taken from the datasheet of the Robotnik RB-VOGUI robot that will be used in IntCDC. The speed of 0.66 m/s is the slowest possible constant speed of the rotating arm in the experiments presented in section 3.

The assumption is that the object describes a linear trajectory at constant speed, and the computation is made to highlight the error caused by non-simultaneous measurements in a given interval of time. The time intervals are all in the order of milliseconds due to several reasons. The aim of the RTS network is to provide reliable coordinates in (quasi) real-time with an extrinsic synchronization smaller than 1 ms. The reason for choosing this limit is related to the specified intrinsic synchronization error by the manufacturer for Trimble RTSs that use ATS (Trimble Inc., 2008). An additional request is to hold the influence of the induced errors below one mm, since in this case the influence will be well below the geometric accuracy (cf. Lerke & Schwieger, 2021).

Achieving this, means that even at the highest speed of the manipulator, which is 2.5 m/s in this case, the induced geometric error caused by unsynchronized measurements within 1 ms would be 2.5 mm. Although in real scenarios, the robot will not be moving at this speed, the aim is

still to obtain positioning accuracy in lower mm domain. Therefore, non-simultaneous and synchronized measurements from different RTS should not lead to position errors larger than those caused by random measurement errors.

Table 1 Simultaneity requirements for different speeds to reach 1 mm travelled distance

Definition	lowest robot speed	speed of rotation arm (section 3)	highest robot speed
Velocity [m/s]	0.15	0.66	2.5
Required simultaneity [ms]	< 6.7	< 1.5	< 0.4

For the required simultaneity, the 1 mm requirement is regarded as the possible maximum error caused by the respective synchronization and simultaneity deviation. This is equivalent to the travelled distance in this time deviation. Table 1 shows that for low velocities of the robot the required synchronization and simultaneity should be less than 6.7 ms. For an average velocity given by the rotation arm (described later in Sec. 3) the 1 ms target would be sufficient too. For high speeds the simultaneity should be better than 0.4 ms.

In case that the 1 ms target for the simultaneity is the overall goal, one may have a look at the reached travelled distance for the same velocities as in Table 1. The relationship is linear and for 0.15 m/s, the travelled distance is 0.15 mm, for 0.66 m/s it is 0.66 mm, and finally for 2.5 m/s, it reaches 2.5 mm. In case of maximum robot speed, the travelled distance is larger than 1 mm and therefore would be at the same level as the geometric accuracy.

3. EXPERIMENTS AND ANALYSIS FOR A NETWORK OF TRIMBLE S7 RTSs

To fulfill the aforementioned requirements, the RTS network was tested in experiments that resemble real positioning scenarios in robotics. The experimental setup was carried out in the measurement laboratory of the IIGS with the four RTS (Fig. 2a & 2b). Multiple trials were conducted to verify either the geometric or the time quality of the streamed data while the RTSs are tracking a reflector. The platform used for moving the reflector is a rotation arm on which the reflector can be fixed. This is a typical test scenario with RTS (cf.; Lackner and Lienhart, 2016; Stempfhuber and Sukale, 2017; Kleemaier, 2018; Thalmann and Neuner, 2021; Vogel, van der Linde and Hake, 2023). As the reflector is rotated on the end of the robotic arm, it describes a circular trajectory situated approximately in a horizontal plane. The orientation is not relevant, because the reference geometry of the position holding the reflector is determined with the laser tracker in the same coordinate system using the tracker active target (Fig. 2c). This is necessary for the upcoming geometric evaluation of the RTS network positioning in post processing. Note that it is impossible to measure both the active target and reflector with the RTSs and laser tracker simultaneously and a joint analysis of both temporal and geometric quality cannot be performed. Therefore, the inevitable constant height offset between active target and reflector (Fig. 2d) must be applied in post-processing.

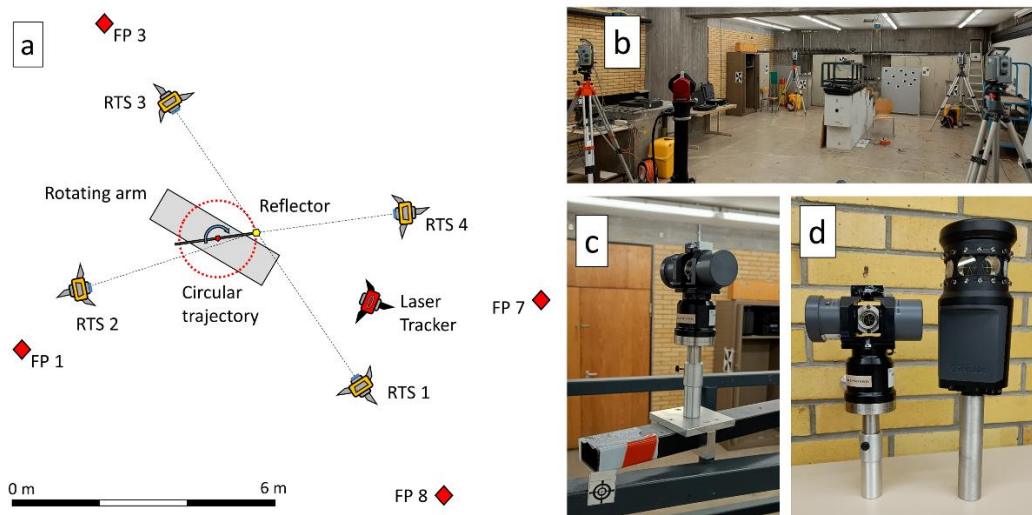


Figure 2 Setup and instruments used in the test scenarios: a – scaled overview of the measurement setup with 4 Trimble S7 RTSs, 4 reference points (FPx) and schematic representation of the rotation arm; b – view of the real setup; c – active target used for the laser tracker measurements mounted on the rotation arm; d – side-by-side representation of the active target for laser tracker and multitrack target for RTS measurements.

All RTSs and the laser tracker are measuring in the same coordinate system after they were positioned by free stationing using the same fix points in the measurement laboratory (Fig. 2a). These fix points are magnetic nests that permit mounting 1.5” reflectors for both tracker and RTS. Their precisely known coordinates originate from a network adjustment based on both laser tracker and total station observations. As an indicator for the quality of the free stationing, the residuals can be representative. In case of the RTS, the residuals are in lower sub-mm domain varying from 0.2 mm to 0.5 mm. For the laser tracker these are all around 0.1 mm. By this, it can be assumed that no systematic errors are introduced due to the used geodetic datum. The reference circle described by the rotating arm is created using a least-square circle fit in the software used to obtain data from the laser tracker, Spatial Analyzer. The circle is fitted based on single points measured with the active target in 5 mm steps. As an indicator for the fit quality, the RMS reached 70 μm , and an absolute value for the radius of 0.900090 m was achieved. This circle is further used as reference for all geometric comparisons of the RTS measurements in section 3.2.

All trials are realized in the setup described above within one day. All instruments passed a warm-up phase of more than one hour before the measurements (Reiterer & Wagner, 2012).

3.1 Verifying time consistency

A first experiment analyzed the time consistency of the entire system while streaming data. Three scenarios are defined for this purpose. First individual time stamps of each RTS are analyzed (Sec. 3.1.1). Next, the synchronization and simultaneity of all RTS time stamps are analyzed in tracking mode (Sec. 3.1.2) and afterwards in angle inquiry mode (Sec. 3.1.3).

3.1.1 RTS individual time

The S7 allows streaming of angles and distances in two modes, 10 Hz and 20 Hz. This means that the sampling intervals between single measurements should ideally be 100 ms for 10 Hz and 50 ms for 20 Hz. This was tested for each RTS individually in order to detect if one or more RTS streams data at the same rate and if there are any differences while the reflector is static or moving. Short intervals of 5 minutes for each trial have proved to be sufficient for this analysis. Longer intervals (e.g. 1 hour) did not show any effects like drifts or inconsistencies in the individual time stamps. Trials 1 and 2 are performed in static mode, therefore the reflector does not move during the experiment duration. Trials 3 and 4 are performed while the reflector is moving at constant speed of 0.66 m/s (2.4 km/h) on the rotation arm.

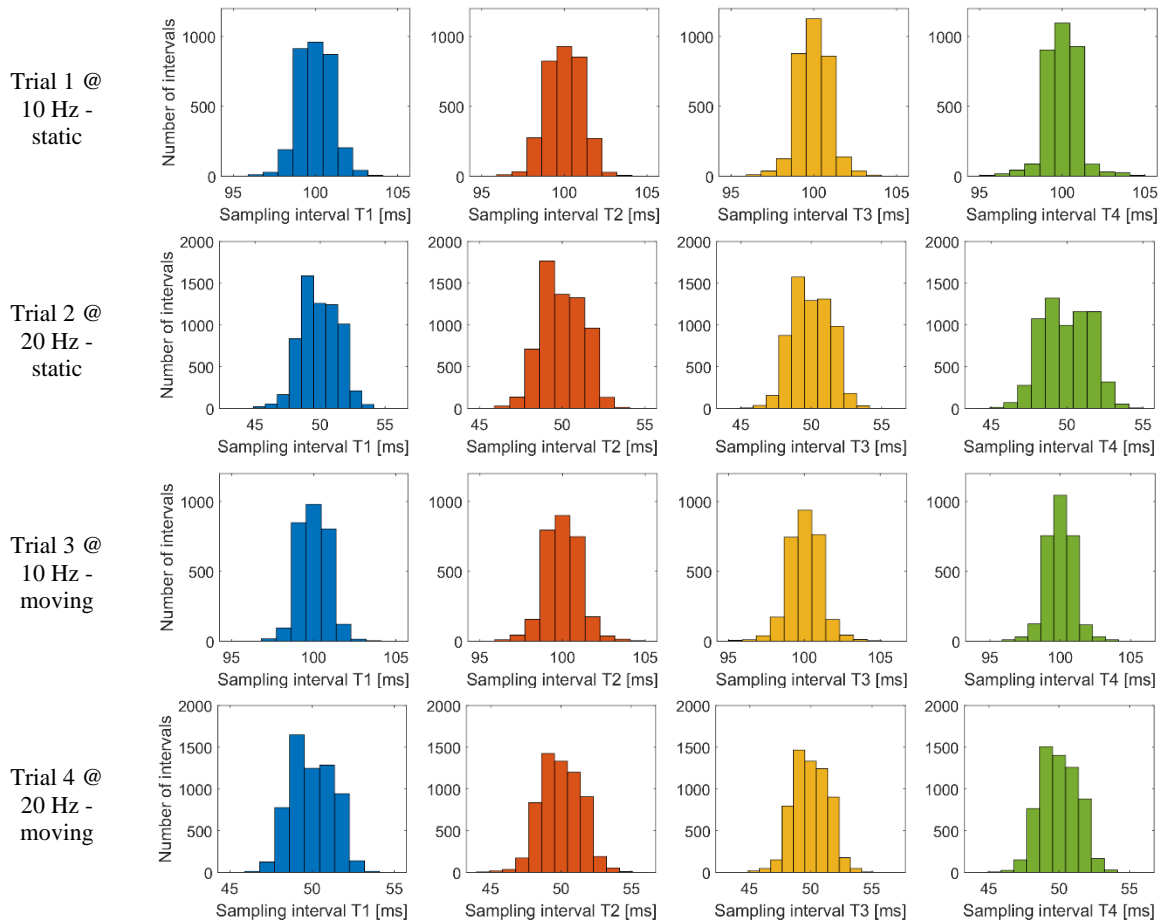


Figure 3 Individual RTS time analysis. Each RTS is depicted by T1 to T4 and the results are represented as histograms.

For all four RTS, the mean sampling interval and standard deviations are given in table 2, while figure 3 illustrates the distribution of sampling intervals. Additionally, the percentage of sampling intervals that fall within ± 1 ms quantile from the expected value (100 ms and 50 ms) is given. This is related to the arguments mentioned in section 2.2.

In the first trial, the mean value of the sampling interval is distributed around 100 ms. Judging only by the mean and standard deviation, it can be seen that the standard deviation is in all cases larger than the set goal of 1 ms.

However, if a separation is made based on the ± 1 ms quantile, one can affirm that more than 80% of the sample intervals fall within the desired interval.

The second trial resulted in sampling intervals distributed around 50 ms, but there are differences in the distribution form and if judging only by mean and standard deviation, the results seem comparable with the previous trial. Nevertheless, if the previously mentioned separation is made, only 54% to 69% of the data is in the aimed interval. This is a first indicator, that streaming with 20 Hz is less reliable than the other streaming mode.

Trials 3 and 4 show similar patterns and there is no apparent difference in the sampling interval quality if the reflector is moving or not. With exception of T4 for trial 4 and 2, comparable values were achieved.

Table 2 Percentage of data within ± 1 ms from sampling rate, mean and standard deviation

Trial no./TS no.	T1	T2	T3	T4
Trial 1 @ 10 Hz - static	84.7 % 100.0 \pm 1.2	80.4 % 99.9 \pm 1.2	88.4 % 100.0 \pm 1.1	90.4 % 100.0 \pm 1.1
Trial 2 @ 20 Hz - static	63.3 % 50.0 \pm 1.6	69.0 % 49.9 \pm 1.4	64.6 % 50.0 \pm 1.5	53.9 % 49.9 \pm 1.7
Trial 3 @ 10 Hz - moving	90.8 % 100.0 \pm 1.0	84.2 % 99.9 \pm 1.2	84.2 % 100.0 \pm 1.2	88.1 % 100.0 \pm 1.1
Trial 4 @ 20 Hz - moving	67.3 % 50.1 \pm 1.4	63.7 % 49.9 \pm 1.6	65.1 % 50.0 \pm 1.6	67.1 % 50.0 \pm 1.5

It can be affirmed that the mean value for the sampling interval for both 10 Hz and 20 Hz adhere with the expected ones. There is also no noticeable difference for the sampling intervals if the tracked reflector is static or moving. However, there is a qualitative loss if streaming with 20 Hz compared to 10 Hz.

3.1.2 RTS network time in tracking mode

Data from the previous four trials is now used for another purpose. By network time, the absolute time stamps are analyzed. These time stamps from all four RasPis are retrieved in UNIX format (seconds since 01.01.1970 UTC) with μ s resolution. In all further figures, they were formatted for better readability. Before the measurements can start, all four RTS have a search phase in which the multitarget is found. Since the multitrack MT1000 is an active target, a unique identifier is set and the incorporated LEDs transmit a unique light code, therefore the RTS tracks only the chosen target. Other reflectors that may come in the field of view of each RTS do not interfere with the measurements. After the multitrack target is locked by all RTS, the user can manually trigger the tracking mode. Note that all measurements are triggered simultaneously in LabView. Therefore, it was expected that all measurements start streaming data at the same time or within the previously found small sampling interval discrepancies.

In figure 3, the time stamps from the firstly available measurements (right after triggering) are shown in parallel. For each RTS, a vertical line depicts the respective time stamp on the same time axis.

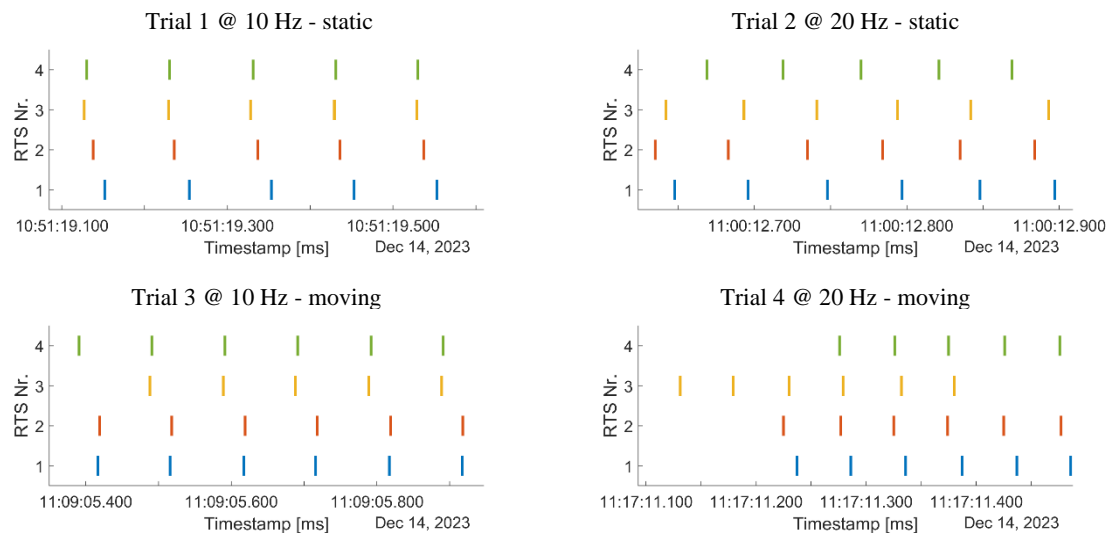


Figure 4 The first time stamps of RTS network after simultaneously triggering the measurement. Each RTS timestamp is depicted by a different color on the time stamp.

A first observation is that the RTSs start measuring at different times, even though they are triggered in the same time. Delays or dead times caused by the software (LabView) can be excluded as explained later in the angle streaming trials. Consequently, the differences between the initial measurements of each RTS must be related to a hardware component of the system. In all four trials and independent of the streaming mode or if the reflector is moving or not, the delays between timestamps have a random character. Initially, the authors hoped that there might be systematic delays, for example RTS 1 is always quicker than RTS 3, and in this case the issue could be solved by implementing an individual timeout after triggering the measurements. Unfortunately, this is not a feasible solution because the delays between the fastest and slowest RTS vary randomly. For the presented trials (Fig. 4), they vary from 25 ms to 145 ms, as already highlighted in table 1. Specifically, in trial 1 the delay is 25 ms between RTS 1 (slowest) and 3 (fastest), trial 2 lead to 34 ms between RTS 4 and 2, trial 3 lead to 97 ms between RTS 3 and 4, and finally, the extreme case, trial 4 to 145 ms between RTS 4 and 3. Additional trials (not shown here) revealed the similar findings in which the delays varied between 39 ms and 139 ms. In section 2, the consequences of such delays were presented in form of distance travelled by an object in the respective time (table 1).

If the intention is to simultaneously measure with all RTSs within delays of less than 1 ms, this approach is definitely unacceptable, because measurements cannot be matched (e.g. in an adjustment) based on time stamps. The assumption is that the delays are caused by the tracking units of the RTS and their individual calibration (cf. Ehrhart and Lienhart, 2017; Schwieger et al., 2020). This is however subject to ongoing research.

3.1.3 RTS network time for angle inquiries

Since multiple RTS are available, an approach based on angular intersection was additionally implemented and tested. Angular readings from the encoders are available quicker than distance

measurements (cf. Lienhart et al., 2017; Gojčič et al., 2017), therefore this feature could be used to eliminate some components of the synchronization issues, intrinsic as well as extrinsic (cf. Sec. 1). In the current publication, the motivation was to verify if the synchronization of angle measurements improves the issues encountered while streaming as seen previously.

In trials 5 and 6, the reflector was moving with the same speed as in trials 3 and 4, while angles were retrieved with 10 Hz, respectively 20 Hz. There is no direct function for streaming angles implemented in the Trimble Linux SDK, therefore, the function for angle inquiry was integrated in a self-developed script. The inquiry was made in LabView on the host laptop with sampling intervals of 100 ms and 50 ms. The time stamp is provided exactly as in the previous cases by the system time of the RasPis updated by the NTP server time as before. This is only valid for angle inquiries, because single distance measurement inquiries are not possible at the same rate (e.g. 10 Hz or 20 Hz).

The delays seen in Fig. 3 for complete measurements do not occur for angular measurements streamed at 10 Hz (Fig. 5). This firstly proves that delays are not caused by the software, therefore triggering measurements simultaneously is possible with 10 Hz. Secondly, it shows that time stamps can be used to match angular observations in contrast to angular and distance observations in this case and with the currently described setup. For trial 6 with measurements streamed at 20 Hz, the delays show a similar pattern only at the beginning of the measurements and then they become larger over time (not represented here). Therefore, angles streamed at 20 Hz cannot be matched based on time stamps for the time being. Further research is necessary to identify the reasons.

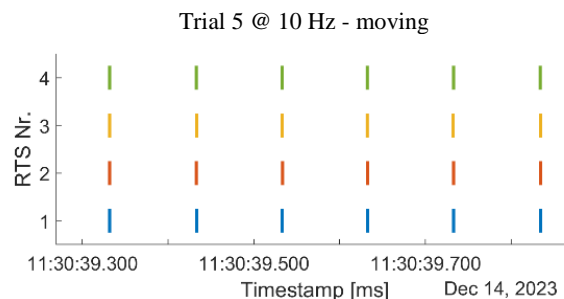


Figure 5 The first time stamps of RTS network after simultaneously triggering angular measurements.

At a closer inspection, there are still small discrepancies between the “fastest” and “slowest” RTS, but they are all under 1 ms. In other words, the first and last measurements of one epoch (e.g. vertical lines in Fig. 5), are less than 1 ms apart from each other. This is not a systematic deviation, since the “fastest” and “slowest” RTS change from time stamp to time stamp, meaning that the deviation has a random character. This corresponds to the set goal of simultaneity. The initial finding was very promising, therefore additional trials (*a* to *n* in table 3) were performed only for this purpose in scenarios with a static and moving reflector. The findings are summarized in table 3. According to these results, the time stamps are not influenced in any way if the observed reflector is static or moving, therefore, judging only from a temporal point of view, the movement (of reflector and implicitly the RTS) is irrelevant.

Table 3 Additional trials for delay determination while streaming angles

Mode	Trial	Max delay (ms)	Mean delay (ms)	Standard deviation (ms)
Static reflector	<i>a</i>	0.423	0.330	0.133
	<i>b</i>	0.145		
	<i>c</i>	0.395		
	<i>d</i>	0.559		
	<i>e</i>	0.164		
	<i>f</i>	0.406		
	<i>g</i>	0.216		
Moving reflector	<i>h</i>	0.241	0.292	0.059
	<i>i</i>	0.365		
	<i>j</i>	0.290		
	<i>k</i>	0.398		
	<i>l</i>	0.238		
	<i>m</i>	0.319		
	<i>n</i>	0.193		

In what concerns the time stamps, all cases show better simultaneous measurements between the observations in the RTS network, compared to those in the streaming mode. In average, the mean delay for static scenarios was 0.33 ms and 0.29 ms in the moving scenario.

3.1.4 Discussion of the temporal quality

Here it should be mentioned, that these values do not include the intrinsic synchronization errors that still have to be treated separately. Therefore, only the results obtained in sections 3.1.1 to 3.1.3 are shortly discussed. The time values represent the smallest and largest delays, between measurements described previously in normal tracking mode. The 0.3 ms value is the best average value for simultaneous measurements (cf. Sec. 3.1.3) with angles only. Table 4 summarizes these specifications together with a statement about the 1 ms and 1 mm requirement presented in Sec. 2.2.

Table 4 Specifications of tracked objects and positioning requirements for objects travelling at these speeds.

Object linear speed [m/s]	Time [ms]	Traveled distance [m]	Temporal requirement 1 ms	Spatial requirement 1 mm
0.15	25	0.004	No	No
	145	0.022	No	No
	1	0.00015	Yes	Yes
	0.3	0.00005	Yes	Yes
0.66	25	0.017	No	No
	145	0.096	No	No
	1	0.00066	Yes	Yes
	0.3	0.00020	Yes	Yes
2.50	25	0.063	No	No
	145	0.363	No	No
	1	0.00250	Yes	No
	0.3	0.00075	Yes	Yes

It can be concluded that simultaneous measurements can be realized for different speeds if the error level induced by a mean delay of 0.3 ms is considered acceptable. In table 4, the speeds that respect the requirements, both temporal and spatial can be directly depicted.

3.2 Geometric quality

Until now, only the quality of the time stamps (temporal quality) was analyzed. In this section, the resulting geometry is analyzed analogue to the previous section based on two approaches. First individual observations of angles and distances from each RTS are shown. Afterwards, combined observations based only on angles from the RTS network are presented. The representative quality indicator is based on distances from the reference circle. Each lateral deviation is represented as a vector pointing towards the center of the circle for points inside the circle or away from the circle center for points outside. The overall quality is discriminated based on the RMS computed with all these lateral deviations as explained next.

3.2.1 RTS individual observations

These results are obtained using streamed observations from each RTS at the same constant speed of 0.66 m/s from trials 3 and 4. However, the emphasis here is on the positioning quality. Data preprocessing or adjustment of the data is not implemented in the current setup, therefore the raw measurements are initially used for computing the RMS and maximal lateral deviation (Max). There are cases in which outliers occur and in the future, an outlier detector is planned for implementation. In the current study, a simple 2σ filter was used in post-processing and outliers were eliminated to exemplify the potential positioning quality with outlier detection. The numeric results are depicted by RMS_f and Max_f in these cases. Figure 6 shows the lateral deviations and quality indicators for each data set from trial 3 and 4.

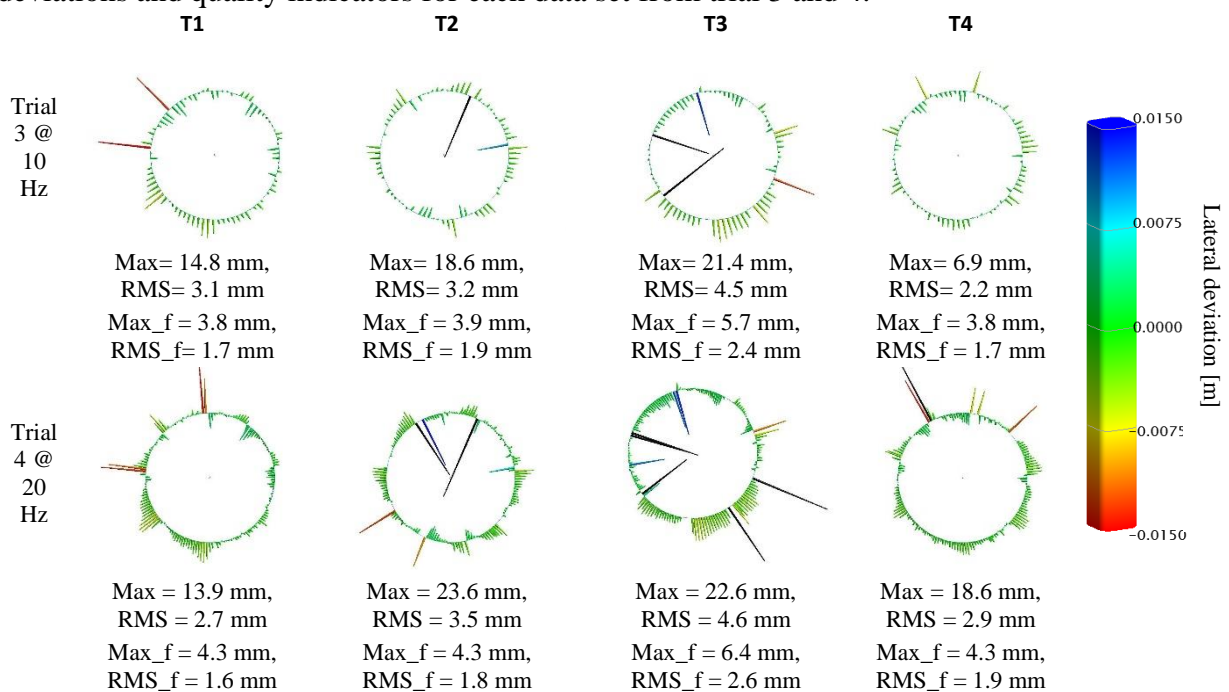


Figure 6 Geometry evaluation of the individual RTS observations in tracking mode with outliers (images), numeric values with outliers (first rows under images), additionally without outliers – no images, only numeric values (second row under images).

During the experiment duration of 5 minutes, the rotating arm moved the reflector several rounds, however, the results presented here show only one round of each data set. Other rounds show similar patterns. A first observation is that the majority of the lateral deviations are in lower mm interval (green color). This is also expected, given the small distances in the laboratory and the known effects of 360° reflectors (Lackner & Lienhart, 2016). In both trials, the RMS is below 5 mm if all lateral deviations are considered. However, in almost all cases, these large lateral deviations can be classified as outliers. If they are eliminated, the RMS values improve and remain around 2 mm.

The largest deviations for each RTS are likewise highlighted below each figure, with and without outlier detection. They reach values up to 23.6 mm without filtering; however, if all lateral deviations that are outside the $\pm 2\sigma$ confidence interval are eliminated, the maximal lateral deviation is generally below 7 mm.

The reason for the occurrence of large deviations remains unclear. It is suspected that they may be caused by mixed signals returning from each RTS, since all four are tracking the same reflector. There may be specific positions of the multitrack reflector in which two RTSs use the same single prisms (of all eight) in the current setup (cf. Fig 2). Another reason may be related to the individual calibration of the fine lock unit of each RTS. However, these are assumptions that can only be verified in further experiments.

In any case, for future developments of the RTS network, a statistical outlier detector will be included in the real-time processing software.

3.2.2 RTS network observations with angles

Unlike in the previous tracking mode where coordinates are determined directly by polar measurements, in these scenarios they are determined based on multiple line intersections. Determining 3D coordinates by line intersection relies on the same working principle as in TMS, however in the current setup it uses more than the minimum two pairs of angles (horizontal and vertical) from two RTS. This translates into an adjustment problem of determining 3D coordinates based on spatial intersection of multiple lines of sight from the four RTSs. The theory behind this approach can be found in many handbooks of geodetic adjustments (cf. Jäger et al., 2006; Niemeier, 2008; Ghilani, 2018).

The currently used adjustment software is Java·Applied·Geodesy·3D (JAG3D), an open source least-squares software package for geodetic sciences (<https://github.com/applied-geodesy/jag3d>). In summary, the 3D coordinates of each point are determined from the intersection of four observations sets, comprised of eight angles (from each RTS one horizontal and vertical angle) per epoch.

In trials 5 and 6 the same data with the reflector moving at constant speed of 0.66 m/s, was used. Note that the angles were streamed as mentioned in Sec. 3 with 10 Hz and 20 Hz respectively. The initially obtained 3D coordinates in both trial showed unsatisfactory results with large systematic deviations from the reference circle. At a closer inspection of the individual measurement data in trial 5 and 6, the following anomalies were observed:

- in trial 5 (10 Hz), although the time stamps indicated that measurements were simultaneously retrieved from the RTSs during the entire trial with 10 Hz, the angular values of each second epoch was a duplicate of the previous one;

- in trial 6 (20 Hz), the time stamps showed simultaneity only for the first couple of seconds and afterwards increased delays were noticed up to 150 ms;
- a similar effect for the angular values was observed in trial 6, however, there were pairs of four identical measurements this time.

This explained the initially obtained low quality of the 3D coordinates (e.g. RMS of 19 mm), because the observations were taken at synchronized and simultaneous time stamps, the actual observations did not correspond to the position of the moving reflector at that point of time. If the duplicated values from trial 5 were eliminated, the RMS improved to 2.7 mm in trial 5 (no outlier elimination) and 2.2 with the same $\pm 2\sigma$ threshold (Fig. 6). Therefore, it can be stated that angle inquiries can be made with a sampling rate up to 5 Hz. Currently, higher rates lead only to apparent measurements. This finding needs to be further investigated.

For trial 6, the same improvement could not be obtained, due to the increasing delays between observations and it could be concluded that a similar effect as in tracking mode with 20 Hz (cf. 3.1.2) occurred here. The consequences are RMS values around 23 mm with the largest deviations of 54 mm. This is unacceptable and further research is needed to explain why this happens at 20 Hz, but does not happen in the 10 Hz case for the time stamps.

It should be noted that these findings apply for the currently developed RTS network and should not be generalized for other RTS networks.

The last two trials were intended to verify the geometric quality at lower speeds than the previous two. Therefore, in trials 7 and 8 the reflector was rotated manually at a much slower non-linear speed. The difference is as before with 10 Hz and 20 Hz sampling rates. Unsurprisingly, the same phenomena with apparent measurements occurred for these trials and it can be stated that it is not related to the speed of the moving object. As before, for the 20 Hz case (trial 8) matching based on time stamps was not possible, therefore, only the results for trial 7 after duplicates elimination are presented (Fig. 7). Opposite to intuition, the RMS and maximal lateral deviation increased if compared to the previous results for constant speed. This may be related to the non-linear speed of the object that leads to non-constant rotation of each RTS. Further trials are necessary to confirm this also for different speeds (cf. Tab. 4).

The ellipse-like deviations from the ideal circle look like typical effects from intrinsic synchronization errors of one RTS. Obviously, this cannot be the reason here and future investigations regarding these systematic effects are essential.

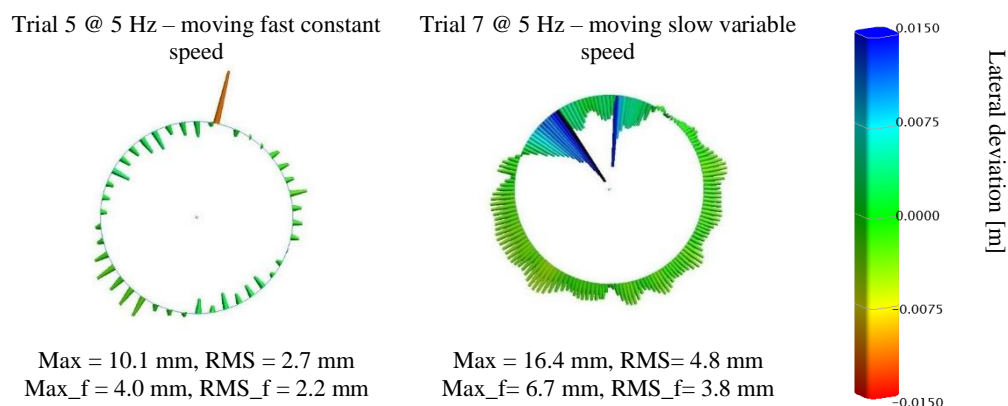


Figure 7 Geometry evaluation of the network RTS observations based on angles intersection.

4. CONCLUSIONS

In conclusion, this publication discusses the possibilities and limitations of extrinsic synchronization and simultaneous measurements in a network of RTSs. The study was motivated by the need to automate processes in the construction industry, particularly the high-precision positioning required for autonomous robots and manipulators on a construction site. The RTS network in question consists of four Trimble S7 RTS that track the same reflector in a given coordinate system. Data communication is based on the Trimble Linux SDK with libraries and scripts in C++. The central host computer uses a custom LabView code (Vi) but the same can be done in any other programming language that supports parallelization. The extrinsic synchronization is achieved using NTP time from a stratum 1 server, which has proven to be a reliable solution.

This paper also analyzes the time consistency in two streaming modes. Results are good for both 10 Hz and 20 Hz modes; however, the authors' recommend choosing the 10 Hz mode since more than 80% of the sampling intervals fall within the interval of $100 \text{ ms} \pm 1 \text{ ms}$ (chosen quantile).

The extrinsic synchronization between measurements is obtained, however, the simultaneity in tracking mode remains challenging due to the randomness of the initial measurements. Despite triggering the measurements at the same time, each RTS starts tracking at slightly different times. Delays can reach up to more than 150 ms, which is larger than sampling intervals at 10 Hz.

The geometric quality was asserted using moving objects at constant speeds. The tests involved reflectors moving on a rotation arm at speeds of 0.66 m/s ($\sim 2.4 \text{ km/h}$) with a precisely known reference geometry determined by laser tracker measurements. Based on individual RTS measurements in tracking mode, RMS values of less than 5 mm were obtained. If outliers are eliminated, the average RMS value drops at 2 mm.

To address the simultaneity issues in tracking mode, only angle measurements were additionally utilized. The simultaneity required for matching measurements is given if compared to the findings in tracking mode. Delays between the fastest and slowest RTS are less than 1 ms and an average delay of 0.3 ms while streaming with 10 Hz can be confirmed. However, in reality measurements are only available with a sampling rate of 5 Hz for the time being and streaming with higher rates lead to duplicated values. The resulting geometry based on adjustment of angular measurements is comparable to the results with polar measurements in tracking mode at the same speeds. This method is promising and may eliminate some issues related to the intrinsic synchronization.

Finally, these findings reflect the current state of the RTS network and should not be generalized for other RTS networks. Further experiments are planned with varying distances and network geometries under different conditions, including outdoor settings. Additionally, different trajectories can be tested as long as a reference can be established for this trajectory, such as a model railway track. Alternatives regarding the time stamps are possible with other sources for the temporal reference frame (e.g. using GPS PPS timestamps), although this is not expected to resolve the current issues.

ACKNOWLEDGEMENTS

The research was conducted as part of the research project RP 16-2 "Robotic Platform for Cyber-Physical Assembly" within the Cluster of Excellence Integrative Computational Design and Construction for Architecture (IntCDC) partially supported by the DFG under Germany's Excellence Strategy—EXC 2120/1—390831618.

REFERENCES

- Axelsson, J. (2007). *Serial Port Complete: COM ports, USB virtual COM ports and ports for embedded systems*. Madison, WI: Lakeview Research.
- Bill, R. (1985). Automatische Meß- und Berechnungssysteme für den Industriebereich. *Allgemeine Vermessungs-Nachrichten*, 1985(6), pp.205–210.
- Corke, P.I. (2017). *Robotics, vision and control: fundamental algorithms in MATLAB®*. Cham, Switzerland: Springer.
- Ehrhart, M. and Lienhart, W. (2017). Object tracking with robotic total stations: Current technologies and improvements based on image data. *Journal of Applied Geodesy*, 11(3). <https://doi.org/10.1515/jag-2016-0043>.
- Ghilani, C.D. (2018). *Adjustment computations: spatial data analysis*. Hoboken, NJ Wiley.
- Gojčič, Ž., Kalenjuk, S. and Lienhart, W. (2017). Synchronization routine for real-time synchronization of robotic total stations. In: *INGEO 2017 7th International Conference on Engineering Surveying, Lisbon, Portugal*. pp.83–91.
- Horeličan, T. (2021). *Position Measurement of Moving Objects Using a Robotic Total Station*. Master Thesis Available at: <https://dspace.vut.cz/bitstream/handle/11012/197059/final-thesis.pdf?sequence=1&isAllowed=y>.
- Jäger, R., Müller, T., Saler, H. and Schwäble, R. (2006). *Klassische und robuste Ausgleichungsverfahren : Ein Leitfaden für Ausbildung und Praxis von Geodäten und Geoinformatikern*. Heidelberg: Herbert Wichmann.
- Jolles, J.W. (2021). Broad-scale applications of the Raspberry Pi: A review and guide for biologists. *Methods in Ecology and Evolution*, 12(9), pp.1562–1579. <https://doi.org/10.1111/2041-210x.13652>.
- Kerekes, G. and Schwieger, V. (2018). Kinematic Positioning in a Real Time Robotic Total Station Network System. In: *6th International Conference on Machine Control & Guidance, Berlin*.
- Kleemaier, G. (2018). Multisensorsystem Totalstation. In: *Proceedings of DVW-Seminar 176 - MST 2018 – Multisensortechnologie: Low-Cost Sensoren im Verbund*. DVW – Gesellschaft für Geodäsie, Geoinformation und Landmanagement e. V., pp.25–32.
- Knippers, J., Kropp, C., Menges, A., Sawodny, O. and Weiskopf, D. (2021). Integratives computerbasiertes Planen und Bauen: Architektur digital neu denken. *Bautechnik*, 98(3), pp.194–207. doi:<https://doi.org/10.1002/bate.202000106>.
- Lackner, S. and Lienhart, W. (2016). Impact of Prism Type and Prism Orientation on the Accuracy of Automated Total Station Measurements. In: *Joint International Symposium on Deformation Monitoring, Vienna, Austria*.
- Lauer, A.P.R., Lerke, O., Blagojevic, B., Schwieger, V. and Sawodny, O. (2023). Tool center point control of a large-scale manipulator using absolute position feedback. *Control Engineering Practice*, 131(2023), pp.105388–105388. <https://doi.org/10.1016/j.conengprac.2022.105388>.
- Lerke, O. and Schwieger, V. (2021). Analysis of a kinematic real-time robotic total station network for robot control. *Journal of Applied Geodesy*, 15(3), pp.169–188. <https://doi.org/10.1515/jag-2021-0016>.

Possibilities and Limitations in the Extrinsic Synchronization of Observations from Networks of Robotic Total Stations (12449)

Gabriel Kerekes and Volker Schwieger (Germany)

FIG Working Week 2024

Your World, Our World: Resilient Environment and Sustainable Resource Management for all

Accra, Ghana, 19–24 May 2024

- Lienhart, W., Ehrhart, M. and Grick, M. (2017). High frequent total station measurements for the monitoring of bridge vibrations. *Journal of Applied Geodesy*, 11(1), pp.1–8. <https://doi.org/10.1515/jag-2016-0028>.
- Martin, J., Burbank, J., Kasch, W. and Mills, D.L. (2010). *Network time protocol version 4: Protocol and algorithms specification*. [online] Internet Engineering Task Force Standard. RFC Editor. <https://doi.org/10.17487/RFC5905>.
- Niemeier, W. (2008). *Ausgleichsrechnung Statistische Auswertemethoden*. Berlin: Walter De Gruyter.
- Reiterer, A. and Wagner, A. (2012). System Considerations of an Image Assisted Total Station - Evaluation and Assessment. *Allgemeine Vermessungs-Nachrichten*, 119(3), pp.83–94.
- Schwieger, V., Kerekes, G. and Lerke, O. (2020). Image-Based Target Detection and Tracking Using Image-Assisted Robotic Total Stations. In: O. Sergiyenko, W. Flores Fuentes and P. Mercorelli, eds., *Machine Vision and Navigation*. [online] Cham: Springer International Publishing, pp.133–169. doi:https://doi.org/10.1007/9783030225872_5.
- Stempfhuber, W. (2004). *Ein integritätswahrendes Messsystem für kinematische Anwendungen*. Deutsche Geodätische Kommission, Reihe C. Nr. 576. Verlag C. H. Beck, PhD Thesis. Technical University of Munich.
- Stempfhuber, W. and Sukale, J. (2017). Kinematische Leistungsfähigkeit der MultiStation Leica MS60. *Geomatik Schweiz: Geoinformation und Landmanagement*, 115(3). doi:<https://doi.org/doi.org/10.5169/seals-685925>.
- Thalmann, T. and Neuner, H. (2021). Temporal calibration and synchronization of robotic total stations for kinematic multi-sensor-systems. *Journal of Applied Geodesy*, [online] 15, pp.13–30. doi:<https://doi.org/10.1515/jag-2019-0070>.
- Trimble Inc. (2018). *Datasheet Trimble S7 total station*. Retrieved November 11, 2018, from: <https://geospatial.trimble.com/products-and-solutions/trimble-s7#product-support>.
- Trimble Inc. (2008) Datenblatt Trimble Universale Totalstation. Retrieved November 25, 2023 from: https://www.sitech.de/fileadmin/sitech-content/Brochures/Brochures_DE/Positionierung/Totalstationen/Datenblatt-SPSx30-UTS.pdf
- Vaidis, M., Dubois, W., Guénette, A., Laconte, J., Kubelka, V. and Pomerleau, F. (2022). Extrinsic calibration for highly accurate trajectories reconstruction. *Proceedings of IEEE International Conference on Robotics and Automation (ICRA 2023)*. London.
- Vaidis, M., Giguère, P., Pomerleau, F. and Kubelka, V. (2021). Accurate outdoor ground truth based on total stations. *Proceedings of 18th Conference on Robots and Vision (CRV)*, pp.1–8. Burnaby.
- Verified Market Reports (2023). *Infrastructure Robotic Total Station Market Size, Growth, Share | Analysis by 2030*. [online] Verified Market Reports® | Get Market Analysis and Research Reports. Available at: <https://www.verifiedmarketreports.com/product/infrastructure-robotic-total-station-market/> [Accessed 8 Jan. 2024].
- Vogel, S., van der Linde, M. and Hake, F. (2023). Development and Validation of an External GPS Time Synchronization for Robotic Total Station Control. In: Wieser, A. (Ed.): *Ingenieurvermessung 23: Beiträge zum 20. Internationalen Ingenieurvermessungskurs Zürich, 2023*. Berlin; Offenbach: Wichmann.

BIOGRAPHICAL NOTES

Dr.-Ing. **Gabriel Kerekes**

2008 – 2012 Politechnica University of Timisoara, Romania – B.Sc. Land Surveying and Cadaster
2012 – 2014 Technical University of Bucharest, Romania – M.Sc. Geodesy and Geomatics
2014 – Master Thesis at the University of Stuttgart, Germany
2014 – 2017 intermetric GmbH, Limburg an der Lahn, Germany
since 2017 University of Stuttgart, Institute of Engineering Geodesy (IIGS) Stuttgart, Germany
2023 – PhD at IIGS, University of Stuttgart.

Prof. Dr.-Ing. habil. **Volker Schwieger**

1983 – 1989 Studies of Geodesy in Hannover
1989 Dipl.-Ing. Geodesy (University of Hannover)
1998 Dr.-Ing. Geodesy (University of Hannover)
2004 Habilitation (University of Stuttgart)
since 2010 Professor and Head of Institute of Engineering Geodesy, University of Stuttgart
2015 – 2018 Chair of FIG Commission 5 ‘Positioning and Measurement’
2016 – 2021 Dean of Faculty of Aerospace Engineering and Geodesy, University of Stuttgart
2019 Dr. h.c., Technical University of Civil Engineering, Bucharest, Romania
2022 Honorary Member of FIG

CONTACTS

Dr.-Ing. Gabriel Kerekes
Prof. Dr.-Ing. habil. Dr. h.c. Volker Schwieger

University of Stuttgart
Institute of Engineering Geodesy
Geschwister-Scholl-Str. 24 D
D-70174 Stuttgart
GERMANY
Tel. + 49/711-685-84051
Email: gabriel.kerekes@iigs.uni-stuttgart.de; volker.schwieger@iigs.uni-stuttgart.de
Web site: <http://www.iigs.uni-stuttgart.de>

Possibilities and Limitations in the Extrinsic Synchronization of Observations from Networks of Robotic Total Stations
(12449)

Gabriel Kerekes and Volker Schwieger (Germany)

FIG Working Week 2024

Your World, Our World: Resilient Environment and Sustainable Resource Management for all
Accra, Ghana, 19–24 May 2024